A Dual Band mm-Wave CMOS Oscillator with Left-Handed Resonator

Sai-Wang Tam, Hsing-Ting Yu, Yanghyo Kim, Eran Socher, M.C. Frank Chang and Tatsuo Itoh

University of California, Los Angeles

Abstract — A new technique using left-handed resonator to generate multi-band mm-wave carrier signal is proposed in this paper. The left-handed resonator exhibits non-linear dispersion characteristic which enables uneven spacing between resonant frequencies. A dual band mm-wave oscillator in 90nm CMOS technology is implemented to demonstrate this new technique. Using a mode selection switch, the proposed oscillator operates at 21.3GHz and 55.3GHz respectively with a total power consumption of 14mW.

***Index Terms* — CMOS, Dual Band, Left-Handed (LH) Resonator, mm-Wave, Oscillator**

I. Introduction

Transmitting tens of Giga-bit/sec data in multiple bands and dynamic switching across tens of gigahertz are becoming more critical for wireless applications such as those of millimeter-wave ISM bands at 24 and 60GHz, Automotive Collision Avoidance at 77 GHz and multi-band RF-interconnects up to several hundreds of Giga-Hertz [1]. It would be desirable to design a multi-band oscillator to cover all or at least part of these frequency bands with fast frequency hopping time, low power consumption and small silicon area.

Traditionally, implementing a frequency source covering a wide range of frequencies can be done by multiplexing several sources on-chip [2,3,4]. However, in mm-wave frequencies, the multiplexer in such a design would require ultra-wide-band output characteristics, from DC to the highest frequency of interest, which may be achieved using a distributed design [5], at the expense of higher noise, higher power consumption and larger area.

An alternative approach is to use a single multi-band oscillator to cover multiple channels, which was demonstrated to yield superior performance [6]. In that approach, direct switching of capacitive and inductive elements is used to change the effective L and C of the VCO tank. However, at mm-wave frequencies, switch loss seriously degrades the overall Q of the LC tank. An alternative to direct multiplexing was proposed using an additional current source switching in a transformer-coupled VCO [7], of which switches between inductors could be avoided. The overall Q was indeed improved, but the additional current source increased the power consumption of the VCO.

At mm-wave frequencies, the use of a λ/4 standing wave resonator becomes more attractive due to smaller size and lower loss. It also leads to the generation of multiple evenly spaced resonant frequencies. However, the inherent even frequency spacing makes it less practical in design.

In this paper, a new technique, left-handed (LH) resonator is presented to implement a multi-band mm-wave oscillator which is capable of generating un-evenly spaced resonant frequencies. Under this new technique, the band selection switches are not located in the signal path which can therefore dramatically reduce the size of switches and improve the overall Q of the resonator. Furthermore, compared to the transformer coupling technique, this new technique only utilizes a single pair of cross-coupled pair as a negative resistor without any additional current consumption. In order to demonstrate the feasibility of this new concept, a dual band mm-wave oscillator using LH resonator at 21GHz and 55GHz is constructed in standard digital 90nm CMOS process.

II. CMOS Left-Handed Material

The LH material is usually referred to artificial structure having negative permittivity (ε) and permeability (μ) simultaneously. It has many unique electromagnetic properties such as reversal of Snell's Law and Doppler Effect. Recently, many novel microwave devices have been developed based on the LH structure [8].

In contrast to LH structure, most of the ordinary microwave components use right handed (RH) structures (e.g. transmission line or stubs) with positive ε and μ. The equivalent circuit model and dispersion diagram of the right handed transmission line (TL) are shown in Fig.1. The equivalent circuit of RH TL consists of a series inductor and a shunt capacitor in each unit cell. Since the RH has a linear dispersion characteristic, the phase shift of the RH TL is also linear. Consequently, the RH standing wave resonator can only support evenly spaced resonant frequencies, $f_o, 3f_o, \ldots, (2n+1)f_o$, which is the case in a λ/4 standing wave differential transmission line resonator.

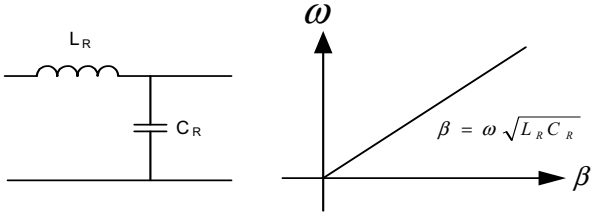

Fig. 1 (a) Equivalent circuit model of a unit cell and (b) dispersion diagram of the RH TL

The equivalent circuit of LH TL unit cell, on the other hand, consists of a series capacitor and a shunt inductor shown in Fig. 2a. As a result, the dispersion characteristic of the LH TL becomes non-linear, which is a unique feature compared with the RH TL, making un-evenly spaced resonant frequencies possible.

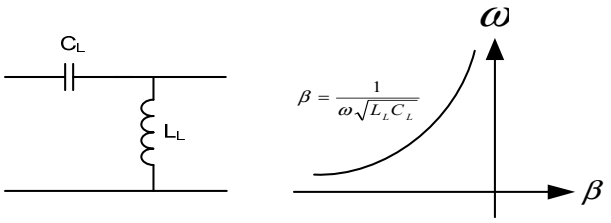

Fig. 2(a) Equivalent circuit model of a unit cell and (b) dispersion diagram of the LH TL

III. Multi-band Resonator Using a LH Structure

With N unit cells of LH structure and negative resistance with a positive feedback loop, a multi-band oscillator can be constructed as shown in Fig.3. Two oscillation criteria are [9]

$$\mathrm{Re}\{Z_{12}\} > mag(-R)$$
$$\mathrm{Im}\{Z_{12}\} = 0$$

The first condition suggests that the negative resistance compensate the loss from the LH structure, the real part of Z_{12} of the LH structure. The second condition is that the total phase shift of one round trip must be equal to $2n\pi$, where n = 0, 1, 2,… Notice that multiple resonant frequencies can be found from the second condition and the dispersion diagram of the N stages of LH unit cell, as shown in Fig. 4. More precisely, N/2 +1 resonant frequencies are observed from the given dispersion curve and N stages of LH unit. The beauty of this approach is that a controllable dispersion curve that can directly control the spacing of each resonant frequency can be created. The drawback of such an approach is the loss and area of the LH resonator. However, in mm-wave frequencies, the size of passive device is relatively small, and both loss and area of the LH resonator can be reduced.

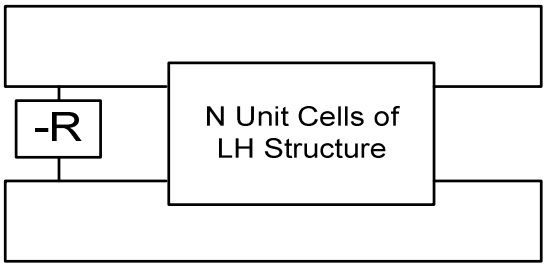

Fig. 3 Conceptual topology of the LH

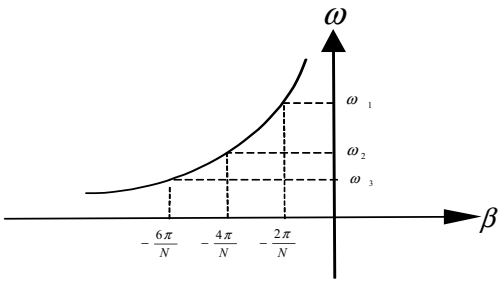

Fig. 4 Dispersion Diagram of the N unit cells LH structure with N resonant frequency

IV. Circuit Design

In order to demonstrate the concept of the multi-band oscillator using LH resonator, an mm-wave CMOS oscillator with dual band, 21GHz and 55GHz, is implemented. The dual band oscillator consists of a cross coupled NMOS pair to act as a negative resistor, two unit cells of an LH structure, and mode selection switches. The schematic of two stages LH resonator is shown in Fig. 5.

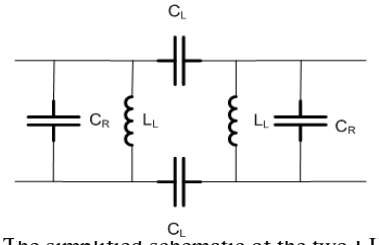

Figure 5 (a) The simplified schematic of the two LH unit cells

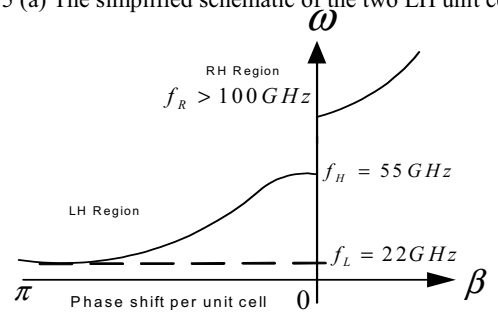

Fig. 5 (b) Two resonant frequencies, 22GHz and 55GHz, are shown in the dispersion diagram of the two LH unit cells. Notice that there is a RH region above the self-resonant frequency of the series capacitor C_L, which is around 100GHz. There is also a bandgap in between two regions, RH and LH.

For this specific two LH unit cell case, two resonant frequencies are

$$f_H = \frac{1}{2\pi\sqrt{L_L C_R}}$$

$$f_L = \frac{1}{2\pi\sqrt{L_L C_R + L_L C_L}}$$

, where C_R is the parasitic capacitance of L_L and the cross-coupled pair transistor.

Based on the dispersion diagram (Fig.5b), the mechanism of oscillation mode selection can be deduced. At the lower resonant frequency (f_L), the phase shift across each unit is π. At the higher resonant frequency (f_H), the phase shift across each unit is zero. A pair of simple and small switches between two unit cells, which are not located on critical signal paths, can achieve the mode selection in such a way that the switches enforce the phase shift in one mode and suppress the other mode. Notice that there is a RH region above the self resonant frequency of the series capacitor C_L, which is around 100GHz. Any signal above 100GHz propagating along the unit cell experiences RH region instead of LH region. In addition, there is a bandgap between two regions, LH and RH, which means any signal with frequency content in this bandgap will be attenuated. It suggests that we can also construct a band-stop filter from this structure. However, in this work, we focus on the multi-band resonator utilizing the LH region only.

The full schematic of the proposed dual band mm-wave oscillator is shown in Fig. 6. When the PMOS mode selection switches are on, due to the differential mode operation, the phase shift across the first unit cell is forced to be π. In the beginning of the oscillation, both oscillation mode f_H and f_L are starting at the same time from the thermal noise level. Since the phase between two unit cell is set to be π during the switches are on, the power of f_L is growing faster and faster and driving the cross-coupled pair to saturation. Eventually, it suppresses the signal in f_H and only f_L survives in the oscillation. On the other hand, when the mode selection switches are off, the phase shift between each unit cell is not limited to any particular value. Therefore, both oscillation modes f_H and f_L compete with each other. In this case, the frequency with lower loss, f_H , dominates the oscillation. In this design, the shunt inductor is 400pH with Q of 17 at 55GHz and Q of 9 at 22GHz, the series capacitor is 50fF, and the size of mode selection PMOS switch is 10μm/0.09μm. The analytic model of the lower resonance mode gives the frequency at 22GHz and the higher resonance mode at 55GHz.

V. Measurement Results

The proposed dual band oscillator is implemented in IBM 90nm standard digital CMOS process. The chip photograph is shown in Fig. 7. The core active area is 150μm × 60μm. When the switch is on, the measured lower resonant frequency, f_L , resonates at 21.3GHz, as shown in Fig. 8a, with the phase noise of -100dBc/Hz at 1MHz offset. When the switch is off, the measured higher resonant frequency, f_H , resonates at 55.5GHz, as shown in Fig. 8b, with the phase noise of -86.7dBc/Hz at 1MHz offset. Table 1 summarizes the measured performance of the proposed dual band oscillator.

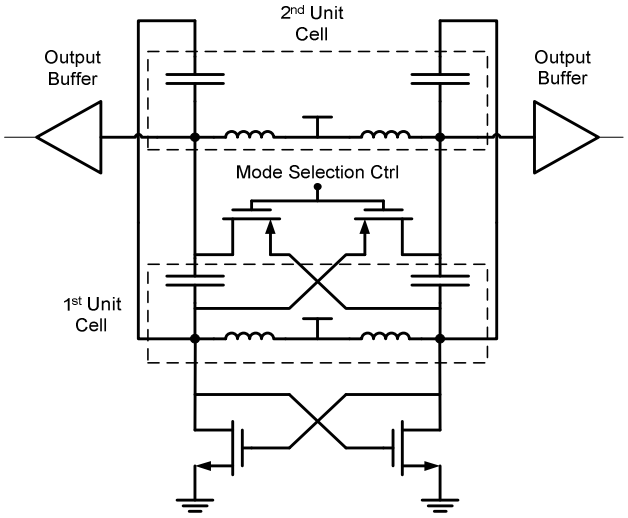

Figure 6 Schematic of the Dual Band mm-wave oscillator using LH resonator

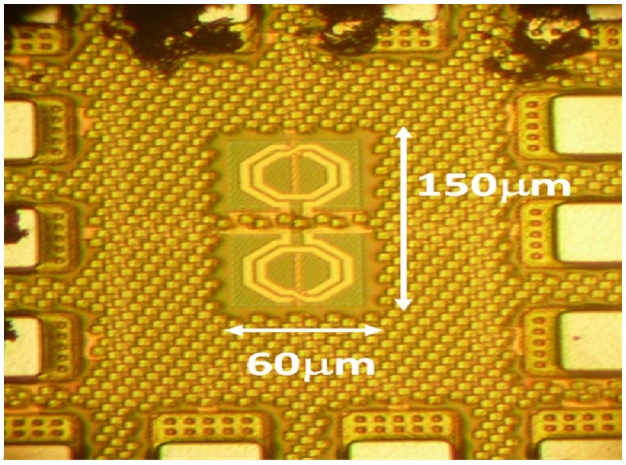

Figure 7 Chip Photograph of the proposed dual band oscillator

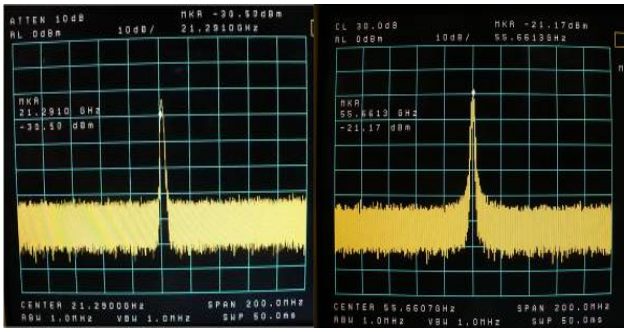

Fig. 8 (a) When the mode selection switches are on, the output frequency is 21.3GHz (b) When the mode selection switches are off, the output frequency is 55.6GHz

Process	IBM 90nm Digital Process
Frequency Band	21GHz and 55GHz
Frequency Switching Range (GHz)	34.3GHz
Frequency Switching Range (%)	62% of highest oscillation frequency
Running at 21GHz Phase Noise @1 MHz offset (dBC/Hz)	-100.8
Running at 55GHz Phase Noise @1 MHz offset (dBC/Hz)	-86.7
VCO-Core Power (mW)	14
VCO-Core Area	150µmX60µm

Table 1: Measurement Summary

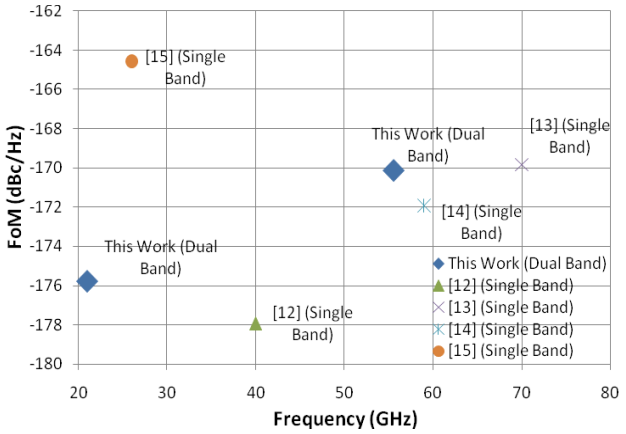

Fig. 9 FOM comparisons of recent published results in MM-wave frequencies.

$FOM = L(f_o)-20\log(f_o/f_{offset})+10\log(P_{dc}/1mW)$

VII. Conclusion

A new design technique on arbitrary multi-band mm-wave oscillator using left-handed resonator is proposed in this paper. A dual band mm-wave oscillator in 90nm CMOS technology has been successfully implemented to demonstrate this new technique. When the mode switch is on, the oscillator operates in lower resonance mode which is at 21.3GHz. When the mode switch is off, the oscillator operates in higher resonance mode which is at 55.3GHz. These switches are located away from critical signal paths and therefore can be made in small size and do not impede the resonator Q. The core area is 150µm × 60µm, and the total power consumption is 14mW.

In contrast to previous work in dual band oscillator [6,7,10], the proposed oscillator can switch between farther band, 21GHz and 55GHz, and achieved the largest frequency switching range, 34GHz. Moreover, this work has comparable FOM with prior work [11,12,13,14] in single band mm-wave oscillator, as shown in Fig. 9.

Acknowledgement

The Authors would like to thank SONY and TAPO for contract and Foundry support.

References

[1] M. Frank Chang et.al, "CMP Network-on-Chip Overlaid With Multi-Band RF-Interconnect," *IEEE HPCA Sym*, Feb. 2008

[2] Alberto Valdes-Garcia et.al, "An 11-Band 3-10GHz Receiver in SiGe BiCMOS for Multiband OFDM UWB Communication," *IEEE Journal of Solid State Circuit*, *Vol. 42, pp 935-948*, April 2007

[3] F. Bohn et.al, "Fully integrated frequency and phase generation for a 6-18GHz tunable multi-band phase-array receiver in CMOS," *IEEE RFIC symposium,* June 2008

[4] O. Werther, et.al, " A Fully Integrated 14 Band, 3.1 to 10.6 GHz 0.13µm SiGe BiCMOS UWB RF Transceiver," *IEEE J. Solid-State Circuits, Vol. 43, pp 2829-2843,* Dec 2008

[5] Amin Arbabian and Ali M. Niknejad, "A Tapered Cascade Multi-Stage Distributed Amplifier with 370GHz GBW in 90nm CMOS," *IEEE RFIC symposium,* June 2008

[6] ZhenBiao Li and Kenneth K. O, "A Low-Phase-Noise and Low-Power Multiband CMOS Voltage-Controlled Oscillator", *IEEE Journal of Solid State Circuit*, *Vol. 40, pp 1296-1302*, June 2005

[7] Burak Catli and Mona M. Hella, " A Dual Band, Wide Tuning Range CMOS Voltage Controlled Oscillator for Multi-band Radio," *IEEE RFIC symposium,* June 2007

[8] Anthony Lai, Christophe Caloz and Tatsuo Itoh, "Composite Right/Left-Handed Transmission Line Metamaterials", *IEEE microwave magazine, Vol. 5, pp 1527-3342*, September 2004

[9] Takashi Ohira, "Rigorous Q-Factor Formulation for One- and Two- Port Passive Linear Networks From an Oscillator Noise Spectrum Viewpoint", *IEEE Transactions on Circuits and Systems-II: Express Briefs, Vol. 52, pp 846-850*, Dec 2005

[10] J. Borremans et.al, "A single-inductor Dual-Band VCO in a 0.06mm^2 5.6GHz multi-band front-end in 90nm digital CMOS," *ISSCC Dig. Tech. Papers, pp. 324-325,* Feb 2008

[11] Jun-Chau Chien and Liang-Hung Lu, " Design of Wide-Tuning-Range Millimeter-Wave CMOS VCO With a Standing-Wave Architecture", *IEEE Journal of Solid State Circuit*, *Vol. 42, pp 1942-1952*, Sept 2007

[12] D. Kim, et.al, "A 70GHz Manufacturable Complementary LC-VCO with 6.14GHz Tuning Range in 65nm SOI CMOS," *ISSCC Dig. Tech. Papers, pp 540-541,* Feb 2007

[13] C. Kao, K.K. O, "Millimeter-Wave Voltage-Controlled Oscillators in 0.13um CMOS Technology," IEEE J. Solid-State Circuits, Vol. 41, pp 1297-1304, Feb 2007

[14] KaChun Kwok, et.al, "A 23 to 29 GHz Transconductor-Tuned VCO MMIC in 0.13um CMOS," *IEEE J. Solid-State Circuits, Vol. 41, pp 2878-2886,* Dec 2007